Cerebral Cortex, October 2017;27: 4677–4690

doi: 10.1093/cercor/bhw261
Advance Access Publication Date: 6 September 2016
Original Article

ORIGINAL ARTICLE

The Role of the Prefrontal Cortex in Action Perception

Vassilis Raos[1,2] and Helen E. Savaki[1,2]

[1]Institute of Applied and Computational Mathematics, Foundation for Research and Technology Hellas, Iraklion, Crete, GR-70013, Greece and [2]Department of Basic Sciences, Faculty of Medicine, School of Health Sciences, University of Crete, Iraklion, Crete, GR-71003, Greece

Address correspondence to Vassilis Raos, Department of Basic Sciences, Faculty of Medicine, School of Health Sciences, University of Crete, PO Box 2208, GR-71003, Iraklion, Crete, Greece. Email: vraos@med.uoc.gr

Abstract

In an attempt to shed light on the role of the prefrontal cortex in action perception, we used the quantitative ^{14}C-deoxyglucose method to reveal the effects elicited by reaching-to-grasp in the light or in the dark and by observation of the same action executed by an external agent. We analyzed the cortical areas in the principal sulcus, the superior and inferior lateral prefrontal convexities and the orbitofrontal cortex of monkeys. We found that execution in the light and observation activated in common most of the lateral prefrontal and orbitofrontal cortical areas, with the exception of 9/46-dorsal activated exclusively for observation and 9/46-ventral, 11 and 13 activated only for execution. Execution in the dark implicated only the ventral bank of the principal sulcus and its adjacent inferior convexity along with areas 47/12-dorsal and 13, whereas execution in the light activated both banks of the principal sulcus and both superior and inferior convexities along with areas 10 and 11. Our results demonstrate that the prefrontal cortex integrates information in the service of both action generation and action perception, and are discussed in relation to its contribution in movement suppression during action observation and in attribution of action to the correct agent.

Key words: action attribution, action execution, action observation, lateral prefrontal cortex, orbitofrontal cortex, principal sulcus

Introduction

The prefrontal cortex (PFC) constitutes the highest level of cortical hierarchy integrating executive information in multiple independent information processing modules (Goldman-Rakic 1996a). The lateral PFC (lPFC), which receives inputs from visual, visuo-motor, somatosensory and auditory association cortices (Barbas and Mesulam 1985), processes information related to working memory, attentional and inhibitory control, mediation of cross temporal contingencies, and active retrieval of memory necessary for executive decisions (Fuster 2001; Petrides 2005). What is not known is whether the PFC subserves action perception/recognition in addition to its documented executive control.

In spite of the considerable number of human neuroimaging studies on action related topics, the involvement of human PFC in action observation remains unclear (Caspers et al. 2010). Explicitly, during action observation and imitation, prefrontal cortical activations were only infrequently reported within the middle frontal gyri (MFG) and inferior FG (IFG) (Gazzola and Keysers 2009; Caspers et al. 2010) or the dorsolateral PFC (dlPFC) (Buccino et al. 2004a, 2004b; Vogt and Thomaschke 2007; Higuchi et al. 2012). Actually it was suggested that the motor representation of an observed action, as provided by the fronto-parietal sensorimotor system, may serve as the 'raw material' for higher order supervisory and monitoring operations by the lPFC (Vogt and Thomaschke 2007; Higuchi et al. 2012).

In the past we demonstrated in the monkey that the observation of an action is neurally represented by a precise association of the movement and its sensory counterparts (kinaesthetic, tactile, and visual), in the same manner as the execution of the action. In fact our studies, which systematically investigated quantitatively and at a high spatial resolution (20 μm) the entire neocortex of the primate brain during execution and observation of the same action, revealed that it is

virtually the same network, which supports both action execution and action observation (Raos et al. 2004, 2007; Evangeliou et al. 2009; Savaki 2010; Kilintari et al. 2011, 2014), rather than a small core circuit of execution related areas (Jeannerod 2001) or the mirror neurons in premotor area F5 and parietal area PF/PFG (Gallese et al. 1996; Fogassi and Luppino 2005) that had been suggested earlier. Moreover, we found that dorsal premotor area F7 is activated for action observation but not for action execution (Raos et al. 2007), contributing to the attribution of action to the correct agent (Savaki 2010). Given that 1) the final functional effect of this area in movement may be inhibitory (Moll and Kuypers 1977; Sawaguchi et al. 1996), and 2) area F7 reaches the spinal cord both directly and indirectly (Keizer and Kuypers 1989), we suggested that an inhibitory input from F7 may suppress overt movements at the spinal level of the observer. This suggestion was further supported by our finding that the spinal forelimb representation is inhibited specifically for action observation (Stamos et al. 2010). The question remains how the premotor cortical area F7 becomes activated and consequently suppresses overt movements during action observation. Our hypothesis is that the activation of area F7 for action observation is mediated via the dlPFC. In fact, a crucial role of the PFC in action suppression was suggested in the past (Lhermitte 1983; De Renzi et al. 1996; Ferrari et al. 2009).

In brief, here we examine whether the PFC integrates information in the service of action observation in addition to its well documented executive control, and whether the PFC contributes 1) to the inhibition of overt movements during action observation and 2) to the attribution of action to the correct agent.

Materials and Methods

Subjects

Twenty five cerebral hemispheres from 13 adult female monkeys (*Macaca mulatta*) weighing between 4 and 6 kg were analyzed in the present study. Animals were purpose-bred by authorized suppliers in Europe (Deutsches Primatenzentum, Gottingen, Germany). Experimental protocols were approved by the animal use committee of our Institute in accordance with European Union regulations concerning biosafety and the use of live animals in research (directive 2010/63/EU and its amendments). Experimental protocols and animal care also accorded with the National Institutes of Health's *Principles of Laboratory Animal Care*. A detailed description of surgical procedures and recordings of electromyographic activity and eye position during the experimental period has been reported previously (Raos et al. 2004, 2007).

In short, for head immobilization a metal bolt was surgically implanted on each animal's head with the use of mandibular plates secured by titanium screws (Synthes, Bettlach, Switzerland) under general anesthesia and aseptic conditions. Analgesics were administered systemically before and after surgery, and monkeys were allowed to recover for at least 3 weeks before the initiation of training. Animals had a water delivery tube attached close to their mouth and were rewarded for correct responses. They were trained to perform their tasks for at least 1 h per day for several months, until they perfected their performance (95% success rate). On the day of the ^{14}C-deoxyglucose (^{14}C-DG) experiment, monkeys performed their tasks uninterruptedly during the 45 min experimental period. Electromyograms recorded from the biceps and wrist extensor muscles (by the use of Ag–AgCl surface electrodes; gain 2000 bandpass filter 0.3–3000 kHz) were previously reported (Raos et al. 2004). Eye movements were recorded with an infrared oculometer (Dr Bouis Devices) and the dwell time of the line of sight as a function of eye position (Raos et al. 2007) as well as the instantaneous eye position as a function of time (Evangeliou et al. 2009) during the critical first 10 min of the ^{14}C-DG experiment, averaged over the monkeys of each group, were previously reported.

Behavioral Tasks

The behavioral apparatus and tasks used in the present study have been reported previously (Raos et al. 2007; Kilintari et al. 2014). In brief, the behavioral apparatus was placed in front of the monkeys at shoulder height, 25 cm away when the monkey had to perform the reaching-to-grasp movements, and 50 cm away when the experimenter had to perform. A sliding circular window of 8° diameter, at the front side of the apparatus, allowed the illuminated object (a horizontally oriented ring) to appear and the subject to grasp it using the hook grip (insertion of its index finger into the ring with pronated hand).

Two monkeys were trained to reach and grasp the illuminated ring with their left forelimbs, whereas their right forelimbs were restricted (El, execution in the light). They had to fixate the illuminated ring for 0.7–1 s, until a dimming of the light would signal reaching, grasping and pulling it with the left forelimb while maintaining fixation. The movement was usually completed within 500–600 ms, while the maximum latency to reach and grasp was set at 1 s. The El monkeys were allowed to move their eyes out of the circular window only during the intertrial intervals (ranging between 2 and 2.5 s).

Three grasping observation (O) monkeys were trained to observe the experimenter performing the same reaching-to-grasp movements with those executed by the El monkeys. We chose a human actor instead of video clips because 1) real actions evoke stronger stimulation and result in a better signal-to-noise ratio than video clips (Caggiano et al. 2011) and 2) monkey and human movements share striking kinesiological similarities (Roy et al. 2000). Both forelimbs of the O monkeys were restricted during the observation training and the ^{14}C-DG experiment. The experimenter was standing on the right side of the monkey and was using the right arm/hand. Both reaching and grasping components of the movement were visible to the monkey. Object and movement parameters as well as intertrial intervals and rate of responses were similar to the ones described for the El monkeys.

Two arm-motion control monkeys had both hands restricted and were trained to maintain their gaze straight ahead during the opening of the window of the apparatus, the presentation of the illuminated object, the closure of the window, and while the experimenter was reaching with extended hand toward the closed window (period ranging between 2.7 and 3 s per trial). Therefore, these monkeys were not exposed to the view of hand preshaping and hand-object interaction (Raos et al. 2014). Two fixation control monkeys were required to hold eye position within a circular window 2.5° in diameter around the fixation target (red circle 1.5° in diameter). We already reported a detailed description of the behavioral apparatus for visual fixation (Savaki et al. 2010; Savaki et al. 2015) and the oculomotor behavior of the arm-motion and the fixation control monkeys (Kilintari et al. 2014; Raos et al. 2014). Comparison of the prefrontal effects in the arm-motion control monkeys with those in the fixation control monkeys revealed no significant increase or decrease of metabolic activity in any prefrontal cortical area (see Table 1 and Fig. 9 in

Table 1 Metabolic effects in the prefrontal cortex of monkeys induced by action execution in the light or in the dark and by action observation

Cortical area	Cl LCGU ± SE	El LCGU ± SE	El/Cl %	O LCGU ± SE	O/Cl %	Cd LCGU ± SE	Ed LCGU ± SE	Ed/Cd %
8 Convexity	56.2 ± 0.7	61.2 ± 0.6	**8.9**	61.2 ± 0.8	**8.9**	52.9 ± 0.8	53.1 ± 0.8	0.4
8 Bank	55.3 ± 0.7	61.8 ± 1.0	**11.8**	64.6 ± 0.8	**16.8**	52.2 ± 1.5	52.6 ± 0.9	0.8
9	46.1 ± 0.6	52.8 ± 0.9	**14.5**	51.2 ± 0.7	**11.1**	45.6 ± 1.2	46.8 ± 0.5	2.6
46 d	47.1 ± 0.8	52.5 ± 0.8	**11.5**	54.9 ± 0.8	**16.6**	44.3 ± 1.0	46.7 ± 0.9	5.4
9/46 d	48.4 ± 0.7	51.3 ± 0.7	6.0	53.7 ± 0.9	**11.0**	48.5 ± 0.7	48.0 ± 0.8	-1.0
46 Principal upper bank	51.3 ± 0.7	58.5 ± 0.7	**14.0**	58.7 ± 0.4	**14.4**	49.2 ± 0.9	52.6 ± 0.5	6.9
46 Principal lower bank	53.8 ± 0.7	61.5 ± 0.9	**14.3**	60.7 ± 0.6	**12.8**	51.7 ± 0.7	56.1 ± 0.5	**8.5**
46 v	52.5 ± 0.7	61.5 ± 1.0	**17.1**	57.4 ± 0.8	**9.5**	51.2 ± 0.4	56.4 ± 0.9	**10.1**
9/46 v	54.8 ± 0.7	62.7 ± 0.9	**14.4**	58.2 ± 0.7	6.2	50.1 ± 1.0	56.8 ± 1.0	**13.4**
47/12 Dorsal	56.5 ± 0.7	64.4 ± 0.9	**14.0**	62.6 ± 0.4	**10.7**	52.5 ± 0.9	57.6 ± 0.8	**9.8**
47/12 Ventral	58.4 ± 0.9	64.0 ± 0.9	**9.5**	66.3 ± 1.0	**13.5**	52.6 ± 0.7	54.7 ± 1.1	4.1
45 Convexity	57.1 ± 0.8	64.6 ± 0.7	**13.1**	64.8 ± 0.7	**13.5**	53.4 ± 0.9	55.1 ± 0.4	3.2
45 Bank	60.9 ± 0.7	66.2 ± 0.6	**8.7**	70.2 ± 0.8	**15.3**	54.5 ± 1.3	57.8 ± 0.6	6.0
10	46.4 ± 0.7	55.4 ± 0.8	**19.4**	51.9 ± 0.6	**11.9**	42.8 ± 1.0	42.8 ± 0.4	0.0
11	48.7 ± 0.8	56.9 ± 0.7	**16.8**	49.0 ± 0.7	0.6	42.8 ± 1.4	44.6 ± 0.7	4.2
13	52.7 ± 0.7	58.8 ± 0.8	**11.6**	55.7 ± 1.0	5.7	46.2 ± 1.0	52.9 ± 1.1	**14.5**

Local cerebral glucose utilization (LCGU) values (mean ± SE in μmol per 100 g per min) in cortical areas of the PFC of monkeys executing or observing reaching-to-grasp movements. Cl values represent the average LCGU values from the 7 hemispheres of the 4 control monkeys in the light. EL values represent the average from the 4 hemispheres of the 2 monkeys reaching-to-grasp in the light. O values represent the average from the 6 hemispheres of the 3 O monkeys observing resching-to-grasp movements. Cd values represent the average LCGU values from the 4 hemispheres of the 2 control monkeys in the dark. ED values represent the average from the 4 hemispheres of the 2 monkeys reaching-to-grasp in the dark. EL/Cf%, O/Cf%, ED/Cd%, percent differences from the corresponding control, calculated as (experimental – control) / control * 100. Values in bold indicate statistically significant differences by one-way ANOVA ($P < 0.05$).

(Raos et al. 2014)). These findings allowed us to pool together the 4 hemispheres of the arm-motion control monkeys with the 3 hemispheres of the fixation control monkeys in a group of 7 hemispheres (Cl, control in the light). Comparisons of the Cl group with the El and the O groups were used to reveal the net effects induced by action execution in the light and by action observation.

Two monkeys were trained to reach and grasp with the left forelimb in complete darkness, while the right forelimb was restricted (Ed, execution in the dark). Accordingly, the monkeys along with the behavioral apparatus were enclosed within black curtains and an extra black drape was positioned in front of the monkey's eyes. Following a low frequency auditory cue (90 Hz), each Ed monkey had to look straight ahead toward the memorized location of the object for 0.7–1 s, until a second high frequency auditory cue (180 Hz) signaled that the monkey had to reach, grasp, and pull the memorized ring with the left forelimb while maintaining its gaze straight ahead. The movement was usually completed within 500–600 ms, while the maximum latency was set to 1 s. The monkeys were allowed to move their eyes only during the 2–2.5 s intertrial intervals.

Finally, 2 control in the dark monkeys (Cd) were presented with acoustic cues similar to those presented to the Ed monkeys. Reward was delivered at random intervals to the Cd monkeys in order to prevent association of the auditory stimuli with the reward expectancy. The total number of rewards that the Cd monkeys received matched that of the Ed monkeys. Detailed description of the task performance and the oculomotor behavior of the Cd and Ed monkeys during the ^{14}C-DG experiment was previously reported (Kilintari et al. 2011).

14C-DG Experiment and Reconstruction of Quantitative 2D-Maps

The ^{14}C-DG method is the only imaging approach to offer direct assessment of brain activity, quantitative measurement of glucose consumption (functional activity) and spatial resolution of 20 μm. Details of the ^{14}C-DG experiment and the brain processing for autoradiography were previously described (Savaki et al. 1993; Raos et al. 2004; Kilintari et al. 2014). In brief, monkeys were subjected to femoral vein and artery catheterization under general anesthesia about 5 h before initiation of the ^{14}C-DG experiment. Plasma glucose concentration, blood pressure and hematocrit were measured to be within normal range. A pulse of 100 mCi/kg of 2-deoxy-D-[1-^{14}C] glucose (specific activity 55 mCi/mmol, ARC) was delivered intravenously, 5 min after the monkeys started performing their tasks. Arterial samples were collected during the succeeding 45 min to measure plasma ^{14}C-DG and glucose concentrations. At 45 min, monkeys were sacrificed by intravenous injection of 50 mg sodium thiopental in 5 ml saline followed by a saturated potassium chloride solution. The cerebral hemispheres were frozen in isopentane at −50°C, and stored at −80°C. About 1000 serial horizontal sections (20 μm thick) were cut in each hemisphere of each monkey, in a cryostat at −20°C. Sections along with precalibrated ^{14}C-standards were exposed to medical X-ray film (Kodak Biomax MR) to prepare autoradiographs. Quantitative densitometric analysis of autoradiographs was performed using the MCID computerized image processing system (MCID, Imaging Research, Ontario, Canada). LCGU values (in μmol/100 g/min) were calculated using the original operational equation of the ^{14}C-DG method (Sokoloff et al. 1977) and the kinetic constants for the monkey (Kennedy et al. 1978). Normalization of LCGU values was based on the averaged unaffected gray matter value pooled across all monkeys (Savaki et al. 1993; Gregoriou and Savaki 2003).

We reconstructed 2D quantitative maps of the spatiointensive pattern of metabolic activity (LCGU values in lmol/100 g/min) in the rostrocaudal and the dorsoventral extent of the PFC in each hemisphere of each monkey, from the autoradiographs of the 20 μm thick horizontal brain sections (Raos et al. 2014). To generate these functional 2D-maps, a data array covering all cortical layers was obtained from each section, by sampling the LCGU values along a rostrocaudal line parallel to the surface of

the cortex. Data arrays from every 5 adjacent autoradiographic sections were averaged (to avoid cutting artifacts) and plotted to produce one line in the 2D-maps of activity. The so generated lines were aligned around a fixed point of alignment to generate a map containing the prefrontal cortical field of interest with labeled surface landmarks (e.g., crowns and fundus of sulci). This way, the dorsoventral sampling resolution of our study equals 20 μm, whereas the dorsoventral plotting resolution of our reconstructed 2D-maps equals 100 μm.

The first reconstructed cortical field contains 1) the lPFC, consisting of a dorsolateral component [areas 8, 9, 10, 46d, and 9/46d (Petrides and Pandya 1999)] and a ventrolateral constituent [areas 9/46 v, 45, and dorsal 47/12 (Petrides and Pandya 2002)]; and 2) the orbitofrontal cortex (OFC), including areas 10, 11, 47/12 v, and 13 (Barbas 2007; Petrides 2007). Each reconstructed 2D-map of the convexity including the lPFC and the OFC was made of 200 lines (1000 sections divided by 5 sections per line). In the 2D-maps, each line represents the average of 5 adjacent serial horizontal sections, extending from the anteriormost point of the brain (anterior tip) until the fundus of the arcuate sulcus. Adjacent lines are aligned around the anterior crown of the arcuate sulcus labeled as 0. (Fig. 1e1). The second reconstructed cortical field contains the cortex within the principal sulcus (PS), which was separately generated based on the same principles. Each 2D-map of the PS contains its dorsal/upper and ventral/lower banks along with the adjoining

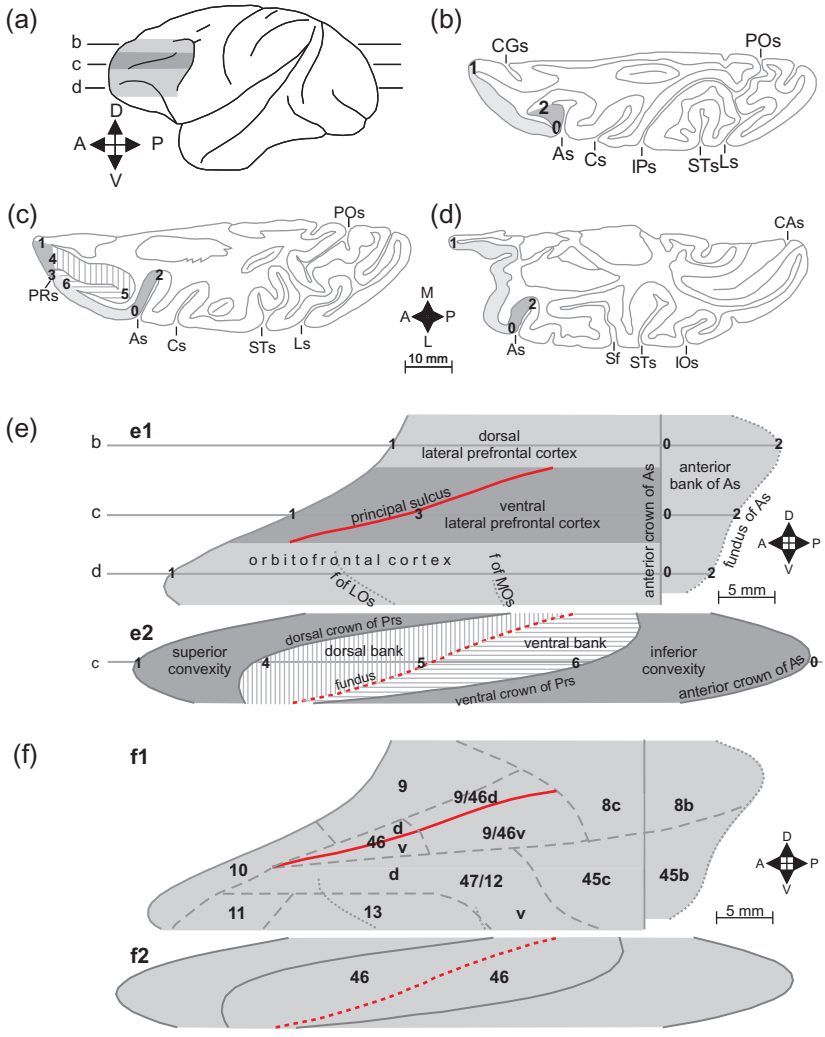

Figure 1. Reconstruction of 2D-maps of the prefrontal cortex. (*a*) Lateral view of the left hemisphere of a monkey brain. Horizontal lines (*b–d*) indicate the 3 different dorsoventral levels of brain sectioning corresponding to the following 3 panels. (*b–d*) Schematic representations of horizontal sections at the dorsoventral levels indicated in panel (*a*). (*e*) Schematic illustration of the geometrically normalized reconstructed cortical field (reference map), which includes the lateral prefrontal/orbitofrontal convexity (e1) and the unfolded principal sulcus (including its dorsal and ventral banks) along with its adjacent superior and inferior convexities (e2), as highlighted by the gray band in panel (e1). Horizontal gray lines (*b–d*) indicate the dorsoventral levels of the sections in the corresponding panels. The vertical line numbered 0 corresponds to the anterior crown of the arcuate sulcus which was used as the point of alignment of adjacent horizontal sections. Numbered lines 1–6 correspond to the numbered tick marks in panels (*b–d*) and illustrate the surface landmarks in both the horizontal sections and the reference 2D-maps. Shaded cortical regions in the 2D-maps of panel e indicate the similarly shaded regions in the horizontal sections of panels (*b–d*). A, anterior; As, arcuate sulcus; CAs, calcarine sulcus; CGs, cingulate sulcus; Cs, central sulcus; D, dorsal; IOs, inferior occipital sulcus; IPs, intraparietal sulcus; L, lateral; Ls, lunate sulcus; LOs, lateral orbital sulcus; M, medial; MOs, medial orbital sulcus; P, posterior; PRs, principal sulcus, POs, parietoccipital sulcus; Sf, Sylvian fissure; STs, superior temporal sulcus; V, ventral. (*f*) Schematic representation of the geometrically normalized 2D-maps in the lateral prefrontal/orbitofrontal cortex (f1) as well as in the cortex of the flattened principal sulcus (f2), with superimposed the borders of anatomical areas. 8b (45b), area 8 (45) in the anterior bank of the arcuate sulcus; 8c (45c), area 8 (45) in the prefrontal convexity; Solid (dotted) lines depict crowns (fundi), dashed lines illustrate the anatomical borders of the cortical areas obtained from the atlas (see methods). The red solid line illustrates the lip of the principal sulcus in the lateral prefrontal convexity (e1, f1), and the red dotted line depicts the fundus of the unfolded sulcus (e2, f2).

opercular cortex, in order to illustrate the extension of activations from the dorsal (ventral) bank into in the superior (inferior) convexities. In these 2D-maps, adjacent anteroposterior sections are aligned around the fundus of the PS (Fig. 1e2). Figure 1 also illustrates the way we reconstructed the corresponding anatomical maps from a brain atlas, to create reference prefrontal maps (see next section). In fact, in order to assign the ^{14}C-DG activations within anatomical areas (in Brodmann areas, BA) we used the combined magnetic resonance imaging (MRI) and histology monkey atlas of Sallem and Logothetis (Saleem and Logothetis 2007). From this atlas, we used horizontal sections of a prefrontal cortical field matching ours, with labeled, not only the surface landmarks (1–6 tick marks in Fig. 1*b–e*), but also the anatomical borders (dashed lines in Fig. 1*f*). We processed these sections from the atlas in the same manner as our autoradiographic sections, in order to generate a 2D-anatomical map equivalent to our 2D-functional maps. After geometrical normalization of all maps (see next section), the corresponding anatomical (from the atlas) and functional (from our study) reconstructed 2D-maps could be superimposed based on their common surface landmarks, and therefore activations could be assigned to BAs. Nomenclature of prefrontal areas was based on Petrides and Pandya (Petrides and Pandya 1994).

The medial cortex dorsal to the corpus callosum has been analyzed and presented in a previous report (Raos et al. 2007). The medial cortex ventral to the corpus callosum displayed several artifacts due to the large surface of the sections (approximate dimensions: 5 cm in the mediolateral axis, 7 cm in the anteroposterior axis) cut from the medial to the lateral side of the hemisphere. The relevant data were analyzed but the resulting maps were not reliable due to the artifacts in the medialmost part of the sections.

Geometrical Normalization of the 2D Anatomical and Functional Maps

In order to be able to compare reconstructed 2D-maps obtained from different hemispheres and animals despite inter- and intra-hemispheric variability, the individual functional and anatomical 2D-maps were processed to match a reference map. The tick marks (1–6 in Fig. 1*b–d*) in each horizontal section, labeling the surface landmarks of the brain such as the frontal tip, crowns, and fundus of sulci, were used for the geometrical normalization of the individual functional and anatomical reconstructed maps (Raos et al. 2014).

For the lPFC, the section by section distances between 1) the anterior tip of the brain and the crown of the PS, 2) the latter and the anterior crown of the arcuate sulcus (As), and 3) the latter and the fundus of the As were measured. The average of each one of these measures was separately computed from all 25 hemispheres to produce a reference map of landmarks. Subsequently, each individual LCGU-map with its own landmarks was linearly transformed in Matlab (MathWorks, Natick, MA) to match the reference map of landmarks. For the OFC, the section by section distances between 1) the tip of the brain and the fundus of the lateral orbital sulcus, LOs; 2) the latter and the fundus of the medial orbital sulcus, MOs; 3) the latter and the anterior crown of the As or its ventral projection; and 4) the latter and the fundus of the As were measured in autoradiographic sections. The orbitofrontal reference map was generated in the same manner as the lateral prefrontal one. The so generated prefrontal cortical reference map of landmarks (including the lPFC and the OFC; Fig. 1e1) was used for geometrical normalization of all the prefrontal cortical maps of all 25 hemispheres. For the reference map of the flattened PS, the section by section distances used were those between 1) the crown of the dorsal bank and the fundus, as well as 2) the fundus and the crown of the ventral bank of the sulcus. The so generated reference map of the PS along with the adjacent superior and inferior convexities is illustrated in Figure 1e2.

To generate the geometrically normalized anatomical map, equivalent to our functional ones, the reconstructed map from the atlas of Saleem and Logotheis (see section above) with its own landmarks was linearly transformed in Matlab (MathWorks, Natick, MA) to match the same reference map of landmarks described above. The latter reconstruction (Fig. 1*f*) contains the anatomical borders of the prefrontal BAs (dashed lines) in addition to the surface landmarks (solid and dotted lines). This way, superimposition of the functional and the anatomical matching maps allows for the macroscopic identification of activated cortical areas. Actually, the transformation of the individual maps to match the reference one may change the total surface of an area. However, the spatial distribution of the activations within each area is preserved because all activations are proportionally shrunk or expanded within its borders.

To obtain average metabolic maps within each experimental group, the LCGU value found in a certain pixel in one of the geometrically normalized 2D-maps of the group was added to the value found in the pixel occupying the same position in all other maps of the same group, and the result was divided by the number of maps used (Fig. 2*a–c*; Fig. 3*a*,*b*). To generate a percent (%) difference map, the LCGU value found in a certain pixel of a geometrically normalized 2D-map of a control hemisphere was subtracted from the value found in the pixel occupying the same position in a similar map obtained from an experimental hemisphere, and their difference was expressed in %LCGU values (Fig. 2*d*,*e*; Fig. 3*c*). Also, to generate maps summarizing the effects of both action execution in the light and action observation (Fig. 2*f*) as well as the effects of action execution in the light and in the dark combined (Fig. 3*d*), we generated reconstructions in which all pixels displaying activity higher than 10% relative to the corresponding pixels of the control map are shown in a different color (red for El, green for O, and blue for Ed), and then, we superimposed them in single maps. Overlap of effects induced by action execution in the light and action observation (Fig. 2*f*) appear yellow (red + green), whereas overlaps between execution in the light and in the dark (Fig. 3*d*) are in pink (red + blue).

Finally, to graphically illustrate the spatiointensive distribution of metabolic activity within each prefrontal cortical area, we plotted the differences between the experimental monkeys and the corresponding control (as %LCGU values and 95% confidence intervals per 100 μm) across the rostrocaudal extent in the reconstructed maps, at different dorsoventral levels (Figs 4 and 5). The plots in these figures represent the percentage differences between the El and the Cl monkeys (red lines), between the O and the Cl monkeys (green lines), and between the Ed and the Cd monkeys (blue lines). Baseline indicates 0% difference from the control. The plots represent differences across specific BAs, as indicated by the ribbon highlighted in the 2D-map above the graphs.

Statistical Analysis

In order to compare statistically the activations among animals, we normalized the metabolic activity by multiplying LCGU values with a factor that was separately determined for

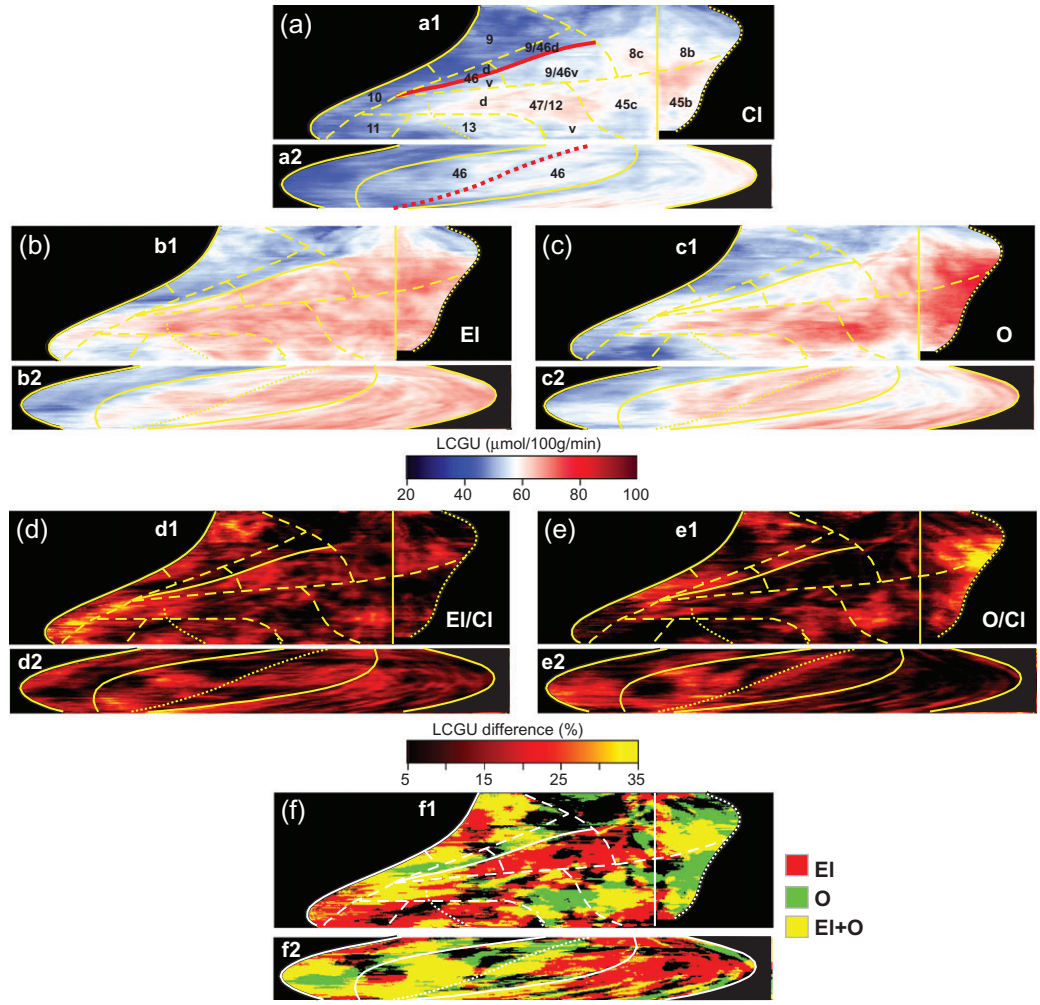

Figure 2. Effects induced by action execution in the light and action observation. (*a*) Quantitative 2D-maps of metabolic activity in the lateral prefrontal/orbitofrontal cortex (a1), and the cortex of the principal sulcus (a2) averaged from the 3 hemispheres of the control Cl monkeys, with the borders of anatomical areas superimposed (dashed yellow lines). (*b*) Averaged 2D-map of activity in (b1) the lateral prefrontal/orbitofrontal cortex, and (b2) the cortex in the principal sulcus, from the 4 hemispheres of the 2 El monkeys. (*c*) Averaged 2D-map of activity in (c1) the lateral prefrontal/orbitofrontal, and (c2) the principal sulcus, from the 6 hemispheres of the 3 O monkeys. Color bar indicates LCGU values in µmol/100 g/min. (*d*) Quantitative maps of net activations induced by reaching-to-grasp in the light in (d1) the lateral prefrontal/orbitofrontal cortex, and (d2) the cortex of the principal sulcus. (*e*) Quantitative maps of net activations induced by observation of reaching-to-grasp movements in (e1) the lateral prefrontal/orbitofrontal cortex, and (e2) the cortex of the principal sulcus. Color bar indicates percentage of LCGU differences from the Cf. (*f*) Superimposition of effects induced by El and O. All significantly activated pixels in the geometrically normalized maps averaged from the 4 El hemispheres are color coded red, and those in the corresponding maps from the 6 O hemispheres are color coded green. The region of overlapping El and O activations is yellow. Other conventions as in Figure 1.

each hemisphere. This factor equals the ratio of the mean LCGU value in unaffected areas (such as the leg and body representations of the primary motor and somatosensory cortices) of the hemisphere in question over the mean LCGU value obtained from the same areas after pooling all hemispheres from all monkeys (Savaki et al. 1993; Gregoriou and Savaki 2003; Picard and Strick 2003). Next, we generated control maps by averaging the geometrically normalized LCGU-maps from the 7 hemispheres of the Cl (Fig. 2*a*) and the 4 hemispheres of the Cd monkeys (Fig. 3*a*). Also, we generated maps from the monkeys grasping in the light, the monkeys observing grasp movements, and the monkeys grasping in the dark by averaging the geometrically normalized LCGU-maps separately from the hemispheres ipsilateral and contralateral to the moving arm in each experimental group. Because the effects in the PFC were bilateral in all experimental groups, both ipsi- and contralateral hemispheres of all animals in each group were pooled for statistical comparisons. Accordingly, El values represent the average LCGU from 4 hemispheres (Fig. 2*b*), O values represent the average from 6 hemispheres (Fig. 2*c*), and Ed values from 4 hemispheres (Fig. 3*b*). The averaged 2D-maps were used for measurement of the LCGU values in each one of the prefrontal cortical areas delineated in Fig. 1*f*. Percent LCGU differences between experimental and control subjects in each one of these prefrontal cortical areas were calculated as (experimental – control)/control × 100 (Table 1). Values in bold in this Table indicate statistically significant differences by one-way analysis of variance (ANOVA) (2 levels: control, experimental; $P < 0.05$).

Results

On the day of the experiment the skeletomotor and oculomotor behavior of the monkeys were constantly recorded, although

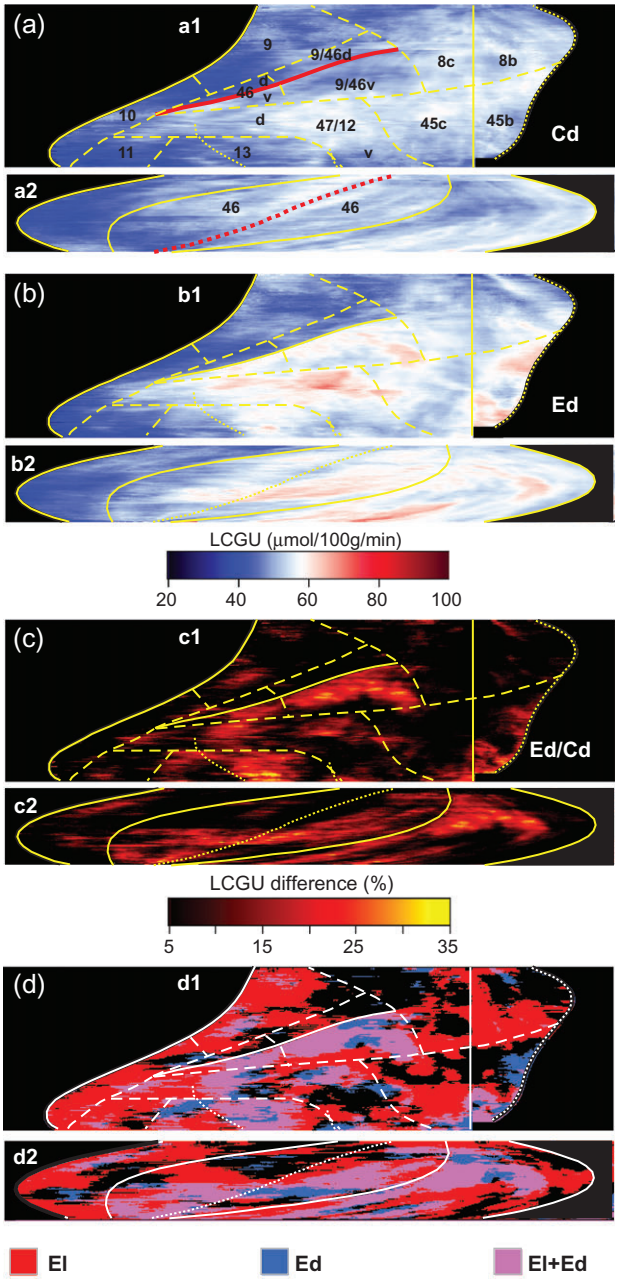

Figure 3. Effects induced by action execution in the dark. (*a*) Quantitative 2D-maps of metabolic activity in the lateral prefrontal/orbitofrontal cortex (a1), and the cortex of the principal sulcus (a2) averaged from the 4 hemispheres of the Cd monkeys, with the borders of anatomical areas superimposed (dashed yellow lines). (*b*) Averaged 2D-map of activity in (b1) the lateral prefrontal/orbitofrontal cortex, and (b2) the cortex in the principal sulcus, from the 4 hemispheres of the 2 Ed monkeys. (*c*) Quantitative maps of net activations induced by reaching-to-grasp in the dark in (c1) the lateral prefrontal/orbitofrontal cortex, and (c2) the cortex of the principal sulcus. (*d*) Superimposition of effects induced by El and Ed. All significantly activated pixels in the geometrically normalized maps averaged from the 4 El hemispheres are color coded red, and those in the corresponding maps from the 4 Ed hemispheres are color coded blue. The region of overlapping El and Ed activations is pink. Other conventions as in Figs 1–2.

85% of the radiolabeled DG is taken up within the first 10 min, which is considered the critical experimental period of time (Sokoloff et al. 1977; Savaki et al. 1980). During the first 10 min of the ^{14}C-DG experiment, the El and the Ed monkeys executed an average of 10 and 11 reaching-to-grasp movements per minute, respectively, while the O monkeys observed an average of 12 reaching-to-grasp movements per minute. The oculomotor behavior of the monkeys was previously reported (see Fig. 1 of (Kilintari et al. 2011)). In brief, all experimental monkeys maintained their line of sight within the window of the behavioral apparatus (8° in diameter) for at least 7 min during the first 10 min of the ^{14}C-DG experiment. During the nonfixating intervals, the animals did not display any systematic oculomotor behavior which could account for false positive effects in oculomotor related areas.

To reveal the prefrontal cortical effects induced by action execution in the light, LCGU values (in micromoles per 100 g per minute) obtained from the monkeys grasping in the light (El) were compared with those obtained from their control (Cl). Figure 2*a* illustrates the quantitative 2D-map of metabolic activity in 1) the prefrontal convexity including the lPFC and the OFC (upper panel) and 2) the PS and its adjacent cortex of the superior and inferior convexities (lower panel), averaged from the 7 hemispheres of the Cl monkeys. In this and the following figures, the PFC reconstructions are presented following the same convention, namely anterior is left and posterior is right. On the other hand, the reconstruction of the PS represents the flattened sulcus, with the anterior part of the 2 banks around the crowns, and the posterior part around the fundus in the middle of the reconstruction (Fig. 1e2). The cortex of the convexity adjacent to the banks of the sulcus was included in the 2D-map in order to illustrate the continuum of the activated regions in and around the sulcus. Figure 2*b* depicts the averaged metabolic maps of the PFC and the PS from 4 El hemispheres. To visualize the quantitative net activations induced by action execution in the light, we subtracted the Cl-map shown in Figure 2*a* from the El-map shown in Figure 2*b*. Significant net activations were measured in all the orbitofrontal and lateral prefrontal cortical areas analyzed, with the exception of area 9/46d which remained unaffected (Fig. 2d; Table 1). Consequently, action execution in the light activates the prefrontal cortical areas 8, 9, 46, 9/46 v, 45, 47/12, 10, 11, and 13, that is, the dorsal-lPFC with the exception of 9/46d, both banks of the PS, the ventral-lPFC, and the OFC.

To reveal the activated areas, which were specifically activated by action observation, we generated an averaged quantitative 2D-map of metabolic activity from the 6 hemispheres of the monkeys observing grasping movements (O-map: Fig. 2*c*), and we compared it with the corresponding control map (averaged Cl-map: Fig. 2*a*). This comparison revealed observation induced significant net activations in all the areas analyzed, with the exception of 9/46 v, BA11, and BA13 that remained unaffected (Fig. 2*e*; Table 1). Accordingly, action observation activates prefrontal cortical areas 8, 9, 46, 9/46d, 45, 47/12, and 10. Figure 2*f* illustrates the spatial relationship of the activated regions in the PFC 1) for action execution in the light in red and 2) for action observation in green. To generate this picture, we color coded red all significantly activated pixels in the geometrically normalized maps averaged from the 4 El hemispheres, that is, all pixels with LCGU values higher than the corresponding Cl ones by 10%. In a similar manner, in the geometrically normalized maps averaged from the 6 O hemispheres we color coded green all the significantly activated pixels. Superimposition of the latter 2 pictures resulted in Figure 2*f*. In this figure, the region of overlapping activations (red + green = yellow) demonstrates that a large portion of the prefrontal cortical neural space is activated in common for execution in the light and observation. It is also apparent that area 9/46 v along with its adjacent region in

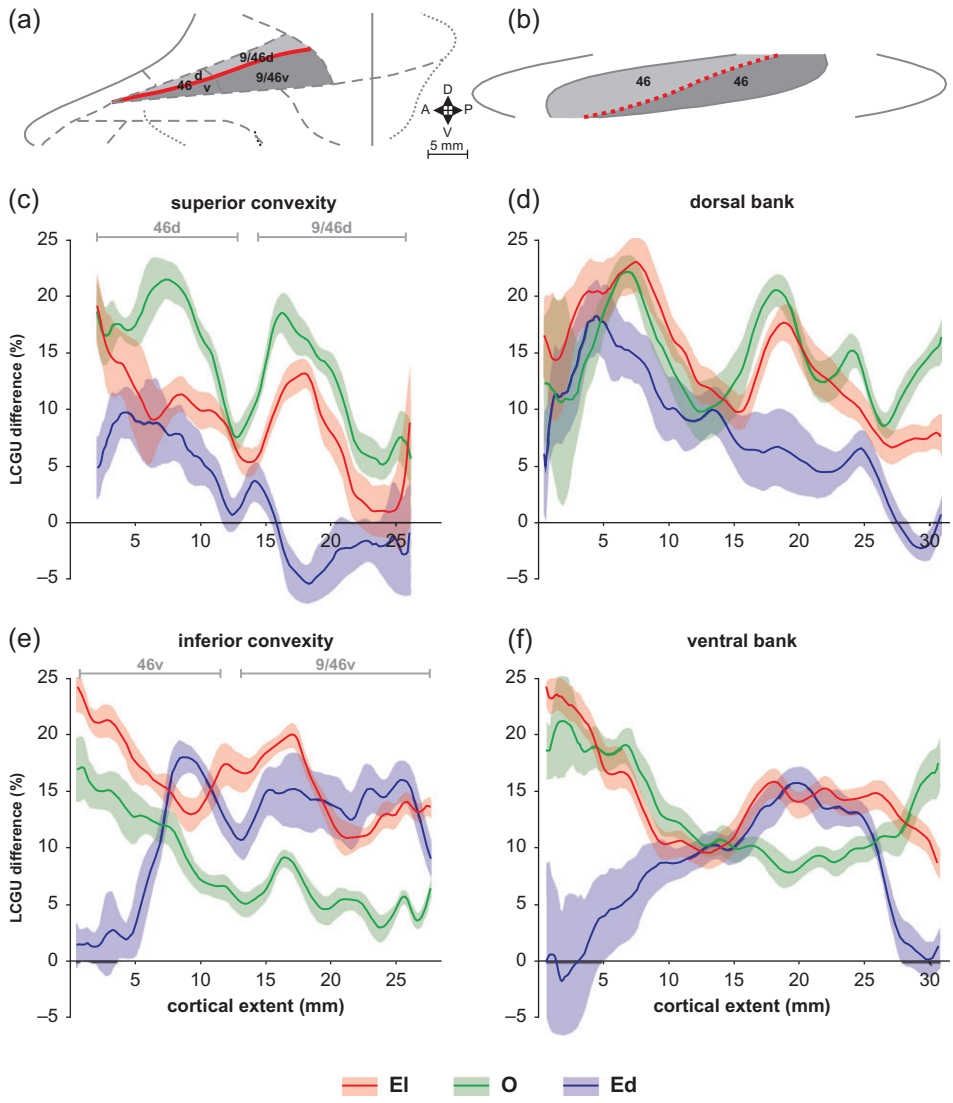

Figure 4. Plots of the distribution of activity throughout the rostrocaudal extent of areas in the dlPFC. (*a*) Illustration of 2 strips (in 2 different gray shades) traversing the superior (light gray) and inferior (dark gray) convexities rostro-caudally. These strips track metabolic effects (average of the %LCGU differences from corresponding controls, and 95% confidence intervals) in the prefrontal cortical areas they go through, with a spatial resolution of 100 μm. (*b*) Illustration of 2 strips traversing the dorsal (light gray) and ventral (dark gray) banks of the principal sulcus rostro-caudally. (*c*) Plots of the %LCGU difference between El and Cl (line in red), O and Cl (line in green) as well as Ed and Cd (line in blue), throughout the anteroposterior extent of areas 46d and 9/46d. Shaded areas around the lines indicate 95% confidence intervals. The extent of areas 46d and 9/46d in the plot is indicated in bracketed lines above the graph and reflected in mm on the abscissa. The ordinate indicates % LCGU difference from the control. (*d*) Plots of the %LCGU difference between El and Cl (red line), O and Cl (green line), Ed and Cd (blue line) throughout the anteroposterior extent of area 46 in the dorsal bank of the principal sulcus. (*e*) Plots of %LCGU difference between El and Cl (red line), O and Cl (green line), Ed and Cd (blue line), throughout the anteroposterior extent of areas 46 v and 9/46 v, with their extent indicated in bracketed lines above the graph. (*f*) Plots of %LCGU difference between El and Cl (red line), O and Cl (green line), Ed and Cd (blue line) throughout the anteroposterior extent of area 46 in the ventral bank of the principal sulcus.

the ventral bank of the PS as well BAs 11 and 13 are activated exclusively by execution (regions in red), whereas a part of 47/12 in the ventral-lPFC and parts of BAs 8 and 45 in the anterior bank of the arcuate sulcus are activated exclusively by action observation (regions in green).

To reveal the prefrontal cortical effects induced by action execution in the dark, LCGU values obtained from the monkeys grasping in the dark (Ed) were compared with those obtained from their corresponding control (Cd monkeys). Figure 3*a* illustrates the quantitative 2D-map of the distribution of metabolic activity in the PFC, averaged from 4 hemispheres of the Cd monkeys. Figure 3*b* depicts the averaged metabolic maps of the PFC from 4 Ed hemispheres. To visualize the quantitative net activations induced by action execution in the dark, we subtracted the map shown in Figure 3*a* from the map shown in Figure 3*b*. Statistically significant net activations induced in the PFC by action execution in the dark were measured in the ventral bank of the PS, areas 46 v and 9/46 v of the inferior convexity, the rostrodorsal part of area 47/12 (47/12d), and BA13 (Fig. 3c; Table 1). Figure 3*d* illustrates the spatial relationship of regions activated for 1) action execution in the light in red and 2) action execution in the dark in blue. Explicitly, in the geometrically normalized maps averaged from the 4 Ed hemispheres all significantly activated pixels (with LCGU values higher by 10% than those of the Cl maps) were color coded blue. Superimposition of the so generated Ed-map on the corresponding map with the El-induced activations color coded red

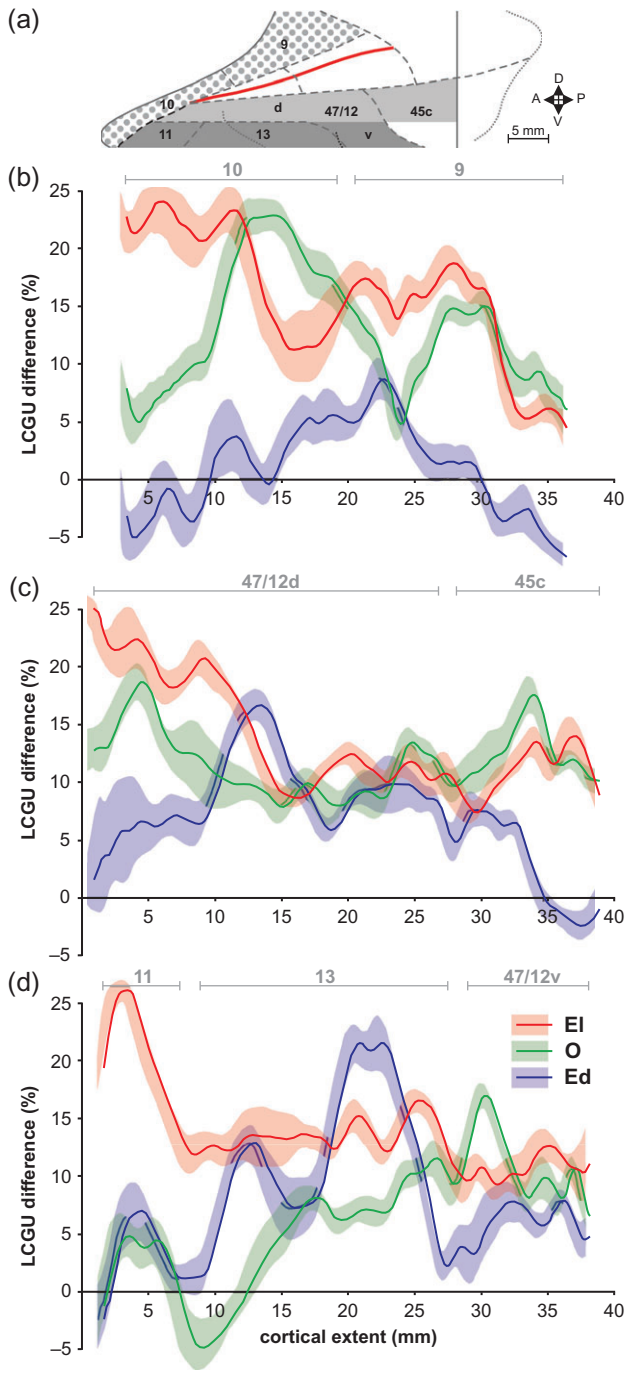

Figure 5. Plots of the activity distribution throughout the rostrocaudal extent of areas in the OFC. (*a*) Illustration of 3 strips traversing the labelled prefrontal cortical areas rostro-caudally. These strips track metabolic effects (average of the %LCGU differences from corresponding controls, and 95% confidence intervals) in the prefrontal cortical areas they go through, with a spatial resolution of 100 μm. (*b*) Plots of %LCGU difference between El and Cl (red line), O and Cl (green line), Ed and Cd (blue line), throughout the anteroposterior extent of areas 10 and 9. Shaded areas around the lines indicate 95% confidence intervals. The extent of areas 10 and 9 in the plot is indicated in bracketed lines above the graph and reflected in mm on the abscissa. The ordinate indicates %LCGU difference from the control. (*c*) Plots of the %LCGU difference between El and Cl (red line), O and Cl (green line), Ed and Cd (blue line) throughout the anteroposterior extent of areas 47/12d and 45c with their extent indicated in bracketed lines above the graph. (*d*) Plots of the %LCGU difference between El and Cl (red line), O and Cl (green line), Ed and Cd (blue line), throughout the anteroposterior extent of areas 11, 13, and 47/12 v, with their extent indicated in bracketed lines above the graph. Other conventions as in Fig. 4.

resulted in Figure 3*d*. The region of overlapping activations (red + blue = pink) demonstrates that a small portion of the prefrontal cortical neural space is activated in common by both conditions of action execution in the light and in the dark. This space covers the ventral bank of the PS along with the contiguous areas 46 v, 9/46 v, 47/12d, and BA13.

Visual inspection of the quantitative averaged 2D-maps of the 3 experimental groups (Fig. 2*b*,*c*; Fig. 3*b*), and the semi-quantitative 2D-maps summarizing the combined effects of El and O combined (Fig. 2*f*) as well as El and Ed (Fig. 3*d*) indicates that the activations within each single affected prefrontal cortical area is not homogeneous. To reveal the local effects pixel by pixel, we graphically illustrated the spatiointensive distribution of metabolic activity along the anteroposterior extent of each cortical area examined. Here, the differences between the experimental monkeys and their corresponding control (as % LCGU and 95% confidence intervals per 100 μm) are plotted across the rostrocaudal extent in the reconstructed 2D-maps (Figs 4 and 5). The ribbons marked in the 2D-maps above the graphs (Fig. 4*a*,*b*) highlight the regions included in the plots, in which 0% represents the baseline and lines in color (red for El, green for O, and blue for Ed) the percentage differences between experimental and control groups (Fig. 4*c*–*f*).

In detail, Figure 4c demonstrates that: 1) The activity within area 46d (left half of the plot) for action execution in the light (Fig. 4c, red line in the left half of the plot) follows a decreasing curve, extending from its rostral most part bordering BA10 (which displays the highest activity in this experimental group: see Fig. 5*b*—red line and Table 1) to its caudal most portion bordering area 9/46d. Most of the points of this curve lie above the line of 10% difference from the corresponding control (see ordinate of graph), indicating an overall significant activation of area 46d for action execution (Table 1: El/Cl% value for 46d). This red line continues in area 9/46d (right half of plot) with a peak of activity which, positioned mostly under the 10% level, does not indicate an overall significant activation of this area for action execution in the light (Table 1: El/Cl%, 9/46d). 2) The distribution of activity in the action observation group (Fig. 4c—green line) displays 2 peaks, one within area 46d and another one in area 9/46d. Both of these peaks lie mostly above the 10% level, indicating significant overall activations in areas 46d and 9/46d for action observation (Table 1). 3) The activity induced by action execution in the dark within these two areas is also not uniform. It is higher in area 46d and lower in 9/46d, but overall unaffected in both these areas (Fig. 4c—blue line; Table 1).

The plots of activity distribution in the dorsal bank of the PS (Fig. 4*d*) reveal that although there is an overall activation induced by action execution in the light (red line) and by action observation (green line), the distribution is not uniform in any of them. Actually, 2 peaks of activity are obvious in both conditions. Interestingly, the anterior peak of activity induced by action observation in the dorsal bank of the PS (Fig. 4*d*—green line) is very similar (in intensity, rostrocaudal position and extent) to that in its adjacent area 46d of the superior convexity (Fig. 4c—green line), and the posterior peak is similar to that in its neighboring area 9/46d of the convexity. In other words, the activation in 2 distinct regions of the superior convexity of the dlPFC continues in 2 adjacent areas of the dorsal bank of the PS, signifying 2 functional modules covering adjoining neural space in the superior convexity and the dorsal bank. Moreover, the curves of activity in the superior convexity (Fig. 4c) and the dorsal bank of the PS (Fig. 4*d*) follow quite similar anteroposterior pattern of distribution for action execution in the light

(compare red lines in Fig. 4*c* and *d*) as well as for action execution in the dark (compare blue lines in Fig. 4*c* and *d*). The latter 2 findings support further our suggestion that there are distinct subregions in the dorsal lPFC which display similar function and cover adjacent cortical areas in and out of the sulcus.

Figure 4*e* demonstrates that, for action execution in the dark (blue line) the activity is smaller anteriorly in area 46 v, increases posteriorly and stays at levels significantly higher than the control (above 10%) throughout area 9/46 v. The activity curve for action observation (green line) follows the opposite pattern, that is, starts 15% higher than the control in the anterior part of 46 v, decreases and plateaus at around 5% throughout 9/46 v. The activity for action execution in the light (red line), although not homogeneous, remains at levels above 10% in both areas 46 v and 9/46 v. The most striking difference between Fig. 4*c* and *e* is that area 46d is activated exclusively for action observation whereas area 46 v is activated exclusively for action execution, both in the light and in the dark (see also Table 1). Figure 4*f* illustrates that the pattern of activity in the ventral bank of the PS, for each 1 of the 3 conditions, is similar to the respective one in the inferior convexity (Fig. 4*e*). Activity for action execution in the light (red line) and for action observation (green line) starts at higher levels anteriorly and decreases to plateau posteriorly, whereas activity for action execution in the dark (blue line) starts at a lower level anteriorly and increases posteriorly, in both the inferior convexity and the ventral bank. Moreover, if we take into account the fact that during action execution in the dark only somatosensory information is available, our finding that the peak of activity in the ventral bank rests around the middle of its anteroposterior extent for the Ed-plot (blue line) is in accordance with the report that mainly the middle ventral bank receives from somatosensory areas PF, 1, 2, and SII-PV (Barbas and Mesulam 1985). In contrast to the similarity of activity patterns in the dorsal bank and the superior convexity, as well as in the ventral bank and the inferior convexity, there is no similarity between the patterns of activity in the dorsal and ventral banks of the PS (compare Fig. 4*d* with Fig. 4*f*). Overall, regions of the superior convexity in the lPFC display similar levels of activity with their adjacent regions in the dorsal bank of the PS. The same applies for regions of the inferior convexity and their adjacent regions in the ventral bank. Yet, this principle of activity-continuum does not apply between dorsal and ventral banks of the PS. In other words, functional modules cover each bank and its adjacent convexity and do not cross the fundus of the sulcus.

Figure 5*b* illustrates the distribution of activity across the anteroposterior extent of BA10 and BA9, as highlighted by the dotted pattern in the 2D-map above the graph (Fig. 5*a*). This graph demonstrates that the pattern of activity distribution in these areas is not uniform, and differs substantially between the El (red line) and O (green line) groups, although there is an overall significant activation of both areas in both conditions (Table 1). Our finding that the rostral part of the frontopolar area 10 is activated for action execution in the light whereas its caudal portion is activated for action observation is in accordance with the report that studies involving mentalizing yield more caudal activations (Gilbert et al. 2006). The Ed plot (blue line) shows that execution in the dark does not induce significant activation in either BA10 or BA9 (Table 1), but also that activity distribution within both these areas is not uniform. Figure 5*c* illustrates the distribution of activity across the anteroposterior extent of areas 47/12d and 45c in the inferior convexity, as highlighted by the light gray ribbon in the 2D-map in the top of the figure (Fig. 5*a*). It shows that the pattern of activity distribution in area 47/12d is similar to that in its neighboring areas (46 v and 9/46 v) in the inferior convexity (Fig. 4*e*), with the single exception of the posterior portion of 47/12d in the action observation group (green line) which is activated in contrast to its adjacent 9/46 v which was unaffected. BA45 in the convexity is activated for the El and O groups but not for the Ed one. Given that during execution in the dark the only available information is somatosensory-motor due to the lack of visual input, the blue-line peaks 1) rostral in the inferior convexity (Fig. 4*e*) and 2) intermediate in area 47/12d (Fig. 5*c*) are well-suited to the report that the rostral part of the inferior convexity and the intermediate part of area 47/12d are connected to hand-related frontal and parietal areas (Gerbella et al. 2013). The finding that visuo-oculomotor areas 8 and 45 (Savaki et al. 2015) are more active during action observation than during execution indicates that the visual stimulus of the reaching/grasping arm/hand of the experimenter is more important than that of the actor, probably because visual is the only available information during observation whereas somatosensory efferent information is additionally available during execution. Finally, Fig. 5*d* illustrates the distribution of activity across the anteroposterior extent of BA11, BA13, and the caudoventral portion of area 47/12 (47/12 v), as highlighted by the dark gray ribbon in the 2D-map in the top of the figure. In the El group, activity is significantly higher (by >10%) compared to the corresponding control (Cl) in all 3 areas, and relatively uniform throughout the anteroposterior extent with the exception of the peak in BA11 (red line). In the O group activity is not homogeneously distributed, and is significantly higher than that in the Cl group only in area 47/12 v (green line). Finally, in the Ed group activity is also not uniformly distributed displaying a peak in BA13 that is the only 1, out of the 3, significantly activated (blue line, Table 1).

Discussion

In the present study, we examined whether the PFC integrates information not only in the service of action execution but also in the service of action observation. We also examined whether the PFC may contribute 1) to the inhibition of overt movements during action observation, despite activation of the motor system in the observer's brain; and 2) to the attribution of action to the correct agent, that is, to the 'self' during execution and to the 'other' during observation.

Our finding that action execution in the dark activates the ventral bank of the PS and its adjacent inferior convexity, but not the dorsal bank and its neighboring superior convexity, is compatible with the general anatomical trend of a difference between dorsal and ventral lateral prefrontal regions and the proposals regarding dichotomous functional organization within the PFC (Macko et al. 1982; Pandya and Yeterian 1985; Goldman-Rakic 1996a, 1996b; Petrides 1996, 2000, 2005; Yeterian et al. 2012). More specifically action execution in the dark, which is guided exclusively by somatosensory information because of the lack of visual input, induced activation of only the ventral bank of the PS, ventral areas 46 and 9/46 and the adjacent dorsal part of area 47/12. These findings are in agreement with previous reports that 1) the ventral bank of the PS receives primarily somatosensory inputs from the rostral parietal and the opercular parietal cortex (Petrides and Pandya 1984; Barbas and Mesulam 1985; Preuss and Goldman-Rakic 1989) and 2) somatosensory cortices project to areas 9/46 v, 46 v, and adjoining area 47/12 (Pandya and Yeterian 1996b;

Barbas 2000). Also, our findings accord well with the reports that 1) the ventral bank of the PS and the inferior convexity display neuronal activity related to motor selection based on remembered information (Hoshi et al. 2000) and 2) the ventrolateral PFC contains sensory, motor, and sensorimotor neurons (Bruni et al. 2015) with the movement related neurons discharging during action execution both with and without visual feedback (Simone et al. 2015).

Interestingly, almost all areas of the PFC activated during visually guided execution of reaching-to-grasp movements were also activated by observation of the same action performed by an external agent. The same pattern of homologous activations for execution and observation of the same action was actually revealed in the entire sensory–motor circuitry supporting action generation, including motor, premotor, somatosensory, and visual primary and association areas (Raos et al. 2004, 2007; Evangeliou et al. 2009; Savaki 2010; Kilintari et al. 2011, 2014). This was the basis of our suggestion that we decode others' actions by activating our own action system, that is, by mentally simulating the observed acts (Gordon 1986; Savaki 2010). The only areas activated for action execution in the light but not for action observation were 9/46 v in the lPFC and 11, 13 in the OFC. In fact, our finding that areas 9/46 v and 13 were activated by both action execution in the light and in the dark, but not by action observation, indicates that these areas are monitoring/manipulating information related to the somatosensory rather than the visual effect of the action. This suggestion is compatible with the report that area 13 receives input from the primary somatosensory cortex (areas 1, 2, 3), and that area 9/46 v is connected with somatosensory areas 1, 2, and SII/PV (Pandya and Yeterian 1996b). On the other hand, the areas activated by both action execution in the light and action observation, but not by action execution in the dark, (i.e., areas 8, 9, 46d, 9/46d, dorsal bank, 45, 10, and 47/12 v) may monitor on-line and manipulate within working memory (Petrides 1994) visual information related to the action during its execution and its observation. Indeed, area 8 receives primarily visuospatial inputs from the parietal cortex (Barbas and Mesulam 1981; Huerta et al. 1987; Andersen et al. 1990; Petrides and Pandya 1999; Petrides and Pandya 2009), and areas 8 and 45 in the arcuate sulcus as well as in the convexity display visuooculomotor activity (Savaki et al. 2015). Also, the visuo-spatial input to areas 9, 46, and 9/46d deriving from temporal, parietoccipital and occipital areas has been documented in the past (Barbas 1995; Pandya and Yeterian 1996b; Yeterian et al. 2012). Finally, our finding that the supramodal frontopolar area 10 is activated for action execution in the light and for action observation, but not for action execution in the dark, is compatible with the report that this area is involved in coordinating attention between externally presented and internally represented information (Burgess et al. 2009 Medalla and Barbas 2014).

We previously demonstrated that the system responsible for understanding the actions of other subjects encompasses the entire brain circuitry that supports action execution, including somatotopic activation of the forelimb representation in the primary somatosensory and motor cortices (Raos et al. 2004, 2007; Evangeliou et al. 2009; Savaki 2010; Kilintari et al. 2011, 2014). A pertinent question was: Why does not activation of the motor system result in overt movements during observation of an action? We found that the dorsal premotor area F7 is activated for action observation but not for action execution (Raos et al. 2007). Given that 1) the final functional effect of this area in movement may be inhibitory (Moll and Kuypers 1977; Sawaguchi et al. 1996) and 2) area F7 reaches the spinal cord both directly and indirectly (Keizer and Kuypers 1989),we suggested that area F7 could be specifically involved in the suppression of the action during its observation, explaining why the observer does not move his hand although his motor system is activated during action observation (Savaki 2010). This suggestion was further supported by our findings that 1) the spinal section representing the forelimb (the cervical enlargement) is activated for action execution and inhibited for action observation (Stamos et al. 2010) and 2) area F7 is activated only by observation of purposeful arm movements and not by the view of a static and aimlessly moving forelimb (Raos et al. 2014). In the present study we found that area 46d is more activated for observation than for execution, and that area 9/46d is the only prefrontal area activated exclusively for observation and not for execution in the light or in the dark (Table 1). Interestingly, the dorsal-dlPF is known to project to the dorsal premotor and the ventral-dlPF to the ventral premotor cortex (Matelli et al. 1986; Barbas and Pandya 1987; Pandya and Yeterian 1996a), with the F7-projection zone occupying the broadest territory in the dorsal-dlPF (Wang et al. 2002). Actually, our finding that the largest peaks of activity were displayed in the rostral part of the dorsal bank and the superior convexity in the O monkeys (Fig. 4c,*d*) is compatible with the report that the F7-projecting cells were found more rostral than the F2 ones in these two areas (Wang et al. 2002). Consequently, a legitimate suggestion would be that area 9/46d, which is activated exclusively for action observation in the present study, may activate area F7 that is also exclusively activated for action observation (Raos et al. 2007), and the latter may indirectly inhibit the spinal cord (Stamos et al. 2010) thus suppressing movements during action observation (Savaki 2010). Interestingly, recent findings indicate that prefrontal pathways interface with laminar-specific neurochemical classes of inhibitory neurons in sensory cortices (Barbas and Zikopoulos 2007).

Another pertinent question is: If the same neuronal circuit is assigned the double-responsibility of execution and observation of an action, how do we attribute actions to the correct agents, that is, to the 'self' during action execution and to the 'other' during action observation? Based on our previous results, we have already provided a possible mechanism related to the differences in intensity and lateralization of activations induced in the brain of the observer as compared to the actor (Raos et al. 2007; Evangeliou et al. 2009). Here we provide an additional/complementary mechanism related to the PFC. Area 9/46d in the dlPFC, which is activated only for action observation in the present study, may monitor and manipulate within working memory information incoming from premotor and posterior cortices related to the mismatch between 1) the mentally simulated/predicted motor command and the recalled/anticipated sensory consequence/end-result of the action (see corresponding somatotopic sensory–motor activations in (Raos et al. 2004, 2007)) and 2) the lack of any actual feedback since there is no movement during observation. This incongruity monitored and manipulated by the dlPFC in working memory may contribute to the attribution of action to the correct agent, that is, to the external subject rather than to the 'self' during action observation. This interpretation of our results is in agreement with the previous suggestion that the experience of ourselves or others as the cause of an action may be based on comparison of motor commands with the reafferent feedback from the moving muscles and the external events caused by these commands (Haggard et al. 2002; Johnson and Haggard 2005). Needless to say that this is not the

first time that the PFC is suggested to be involved in perspective taking and agency attribution (Ruby and Decety 2001; David et al. 2006).

Finally, our finding that the distribution of functional activity in each one of the anatomical areas of the PFC is not uniform (Figs 4 and 5) is in accord with previous studies reporting that sensorimotor information in the PFC is distributed into operations performed in multiple small cortical regions, serving as modules (Carmichael and Price 1994; Goldman-Rakic 1996b). Also, our finding that a single functional module may cover parts of adjacent anatomical areas of the PFC is compatible with the report that each prefrontal cortical area is thought to be derived from and related to its neighbor one (Barbas and Pandya 1989). Accordingly, our finding that modules in the superior (inferior) convexity continue and end within the dorsal (ventral) bank of the PS may signify the corresponding origin of these neighboring areas. These modules may contribute differentially to the overall executive and cognitive motor control of the PFC, and may reflect principles analogous to those predicted from computer models of information processing (Marr 1982).

All in all, the extensive overlap of activations induced by action execution and action observation demonstrates that the PFC integrates information not only in the service of action generation but also in the service of action perception. Furthermore, our findings suggest that the dlPFC may contribute in movement prevention during action observation, and in attribution of action to the correct agent. Finally, our results complement previous studies reporting that information within the PFC is integrated across multiple distinct functional modules.

Notes

This work was co-financed by the European Union (European Social Fund) and the Greek State through the action "ARISTEIA II" of the Operational Programme "Education and Lifelong Learning". We thank Maria Kefaloyianni for proficient support in autoradiographic imaging. M.K. was supported in part by BIOSYS (ΚΡΗΠΙΣ, co-financed by the European Regional Development Fund and the Greek State). The authors declare no competing financial interests. *Conflict of Interest:* None declared.

References

Andersen RA, Asanuma C, Essick G, Siegel RM. 1990. Corticocortical connections of anatomically and physiologically defined subdivisions within the inferior parietal lobule. J Comp Neurol. 296:65–113.

Barbas H. 1995. Anatomic basis of cognitive-emotional interactions in the primate prefrontal cortex. Neurosci Behav Rev. 19:499–510.

Barbas H. 2000. Connections underling the synthesis of cognition, memory and emotion in primate prefrontal cortices. Brain Res Bull. 52:319–330.

Barbas H. 2007. Specialized elements of orbitofrontal cortex in primates. Ann N Y Acad Sci. 1121:10–32.

Barbas H, Mesulam M-M. 1985. Cortical afferent input to the principalis region of the rhesus monkey. Neuroscience. 15: 619–637.

Barbas H, Mesulam MM. 1981. Organization of afferent input to subdivisions of area 8 in the rhesus monkey. J Comp Neurol. 200:407–431.

Barbas H, Pandya DN. 1987. Architecture and frontal cortical connections of the premotor cortex (area 6) in the rhesus monkey. J Comp Neurol. 256:211–228.

Barbas H, Pandya DN. 1989. Architecture and intrinsic connections of the prefrontal cortex in the rhesus monkey. J Comp Neurol. 286:353–375.

Barbas H, Zikopoulos B. 2007. The prefrontal cortex and flexible behavior. Neuroscientist. 13:532–545.

Bruni S, Giorgetti V, Bonini L, Fogassi L. 2015. Processing and integration of contextual information in monkey ventrolateral prefrontal neurons during selection and execution of goal-directed manipulative actions. J Neurosci. 35: 11877–11890.

Buccino G, Binkofski F, Riggio L. 2004a. The mirror neuron system and action recognition. Brain Lang. 89:370–376.

Buccino G, Vogt S, Ritzl A, Fink GR, Zilles K, Freund HJ, Rizzolatti G. 2004b. Neural circuits underlying imitation learning of hand actions: an event-related fMRI study. Neuron. 42:323–334.

Burgess PW, Gilbert SJ, Okuda J, Simons JS. 2009.Rostral prefrontal brain regions (Area 10): a gateway between inner thought and the external world? In: Sebanz N, Prinz W, editors. Disorders of volition. Cambridge, MA: MIT Press. p. 373–395.

Caggiano V, Fogassi L, Rizzolatti G, Pomper JK, Thier P, Giese MA, Casile A. 2011. View-based encoding of actions in mirror neurons of area F5 in macaque premotor cortex. Curr Biol. 21:144–148.

Carmichael ST, Price JL. 1994. Architectonic subdivision of the orbital and medial prefrontal cortex in the macaque monkey. J Comp Neurol. 346:366–402.

Caspers S, Zilles K, Laird AR, Eickhoff SB. 2010. ALE meta-analysis of action observation and imitation in the human brain. Neuroimage. 50:1148–1167.

David N, Bewernick BH, Cohen MX, Newen A, Lux S, Fink GR, Shah NJ, Vogeley K. 2006. Neural representations of self versus other: visual-spatial perspective taking and agency in a virtual ball-tossing game. J Cogn Neurosci. 18:898–910.

De Renzi E, Cavalleri F, Facchini S. 1996. Imitation and utilisation behaviour. J Neurol Neurosurg Psychiatry. 61:396–400.

Evangeliou MN, Raos V, Galletti C, Savaki HE. 2009. Functional imaging of the parietal cortex during action execution and observation. Cereb Cortex. 19:624–639.

Ferrari PF, Bonini L, Fogassi L. 2009. From monkey mirror neurons to primate behaviours: possible 'direct' and 'indirect' pathways. Philos Trans R Soc Lond B Biol Sci. 364:2311–2323.

Fogassi L, Luppino G. 2005. Motor functions of the parietal lobe. Curr Opin Neurobiol. 15:626–631.

Fuster JM. 2001. The prefrontal cortex—an update: time is of the essence. Neuron. 30:319–333.

Gallese V, Fadiga L, Fogassi L, Rizzolatti G. 1996. Action recognition in the premotor cortex. Brain. 119:593–609.

Gazzola V, Keysers C. 2009. The observation and execution of actions share motor and somatosensory voxels in all tested subjects: single-subject analyses of unsmoothed fMRI data. Cereb Cortex. 19:1239–1255.

Gerbella M, Borra E, Tonelli S, Rozzi S, Luppino G. 2013. Connectional heterogeneity of the ventral part of the macaque area 46. Cereb Cortex. 23:967–987.

Gilbert SJ, Spengler S, Simons JS, Steele JD, Lawrie SM, Frith CD, Burgess PW. 2006. Functional specialization within rostral prefrontal cortex (area 10): a meta-analysis. J Cogn Neurosci. 18:932–948.

Goldman-Rakic PS. 1996a. The prefrontal landscape: implications of functional architecture for understanding human

mentation and the central executive. Philos Trans R Soc Lond B Biol Sci. 351:1445–1453.
Goldman-Rakic PS. 1996b. Regional and cellular fractionation of working memory. Proc Natl Acad Sci USA. 93:13473–13480.
Gordon RM. 1986. Folk psychology as simulation. Mind Lang. 1: 158–171.
Gregoriou GG, Savaki HE. 2003. When vision guides movement: a functional imaging study of the monkey brain. NeuroImage. 19:959–967.
Haggard P, Clark S, Kalogeras J. 2002. Voluntary action and conscious awareness. Nat Neurosci. 5:382–385.
Higuchi S, Holle H, Roberts N, Eickhoff SB, Vogt S. 2012. Imitation and observational learning of hand actions: prefrontal involvement and connectivity. Neuroimage. 59: 1668–1683.
Hoshi E, Shima K, Tanji J. 2000. Neuronal activity in primate prefrontal cortex in the process of motor selection based on two behavioral rules. J Neurophysiol. 83:2355–2373.
Huerta MF, Krubitzer LA, Kaas JH. 1987. Frontal eye field as defined by intracortical microstimulation in squirrel monkeys, owl monkeys, and macaque monkeys II. Cortical connections. J Comp Neurol. 265:332–361.
Jeannerod M. 2001. Neural simulation of action: a unifying mechanism for motor cognition. Neuroimage. 14:S103–S109.
Johnson H, Haggard P. 2005. Motor awareness without perceptual awareness. Neuropsychologia. 43:227–237.
Keizer K, Kuypers HG. 1989. Distribution of corticospinal neurons with collaterals to the lower brain stem reticular formation in monkey (Macaca fascicularis). Exp Brain Res. 74: 311–318.
Kennedy C, Sakurada O, Shinohara M, Jehle J, Sokoloff L. 1978. Local cerebral glucose utilization in the normal conscious macaque monkey. Ann Neurol . 4::293–301.
Kilintari M, Raos V, Savaki HE. 2011. Grasping in the dark activates early visual cortices. Cereb Cortex. 21:949–963.
Kilintari M, Raos V, Savaki HE. 2014. Involvement of the superior temporal cortex in action execution and action observation. J Neurosci. 34:8999–9011.
Lhermitte F. 1983. 'Utilization behaviour' and its relation to lesions of the frontal lobes. Brain. 106 (Pt 2):237–255.
Macko KA, Jarvis CD, Kennedy C, Miyaoka M, Shinorada M, Sokoloff L, Mishkin M. 1982. Mapping the primate visual system with the [2-14C]deoxyglucose. Science. 218: 394–397.
Marr D. 1982. Vision. San Francisco: W.H. Freeman.
Matelli M, Camarda R, Glickstein M, Rizzolatti G. 1986. Afferent and efferent projections of the inferior area 6 in the macaque monkey. J Comp Neurol. 251:281–298.
Medalla M, Barbas H. 2014. Specialized prefrontal "auditory fields": organization of primate prefrontal-temporal pathways. Front Neurosci. 8:77.
Moll L, Kuypers HGJM. 1977. Premotor cortical ablations in monkeys: contralateral changes in visually guided reaching behavior. Science. 198:317–319.
Pandya DN, Yeterian EH. 1985. Architecture and connections of cortical association areas. In: Peters A, Jones EG, editors. Cerebral cortex: association and auditory cortices. New York: Plenum. p. 3–61.
Pandya DN, Yeterian EH. 1996a. Comparison of prefrontal architecture and connections. Philos Trans R Soc Lond B Biol Sci. 351:1423–1432.
Pandya DN, Yeterian EH. 1996b. Morphological correlations of the human and monkey frontal lobe. In: Damasio AR, Damasio H, Christen Y, editors. Neurobiology of decision making. Berlin Heidelberg: Springer-Verlag. p. 13–46.
Petrides M. 1994. Frontal lobes and working memory: evidence from investigations of the effects of cortical axcisions in nonhuman primates. In: Boller F, J. G, editor. Handbook of neuropsychology. Amsterdam: Elsevier. p. 59–82.
Petrides M. 1996. Specialized systems for the processing of mnemonic information within the primate frontal cortex. Philos Trans R Soc Lond B Biol Sci. 351:1455–1461; discussion 1461-1452.
Petrides M. 2000. Frontal lobes and memory. In: Boller F, Grafman J, editors. Handbook of neuropsychology. Amsterdam: Elsevier. p. 67–84.
Petrides M. 2005. Lateral prefrontal cortex: architectonic and functional organization. Philos Trans R Soc Lond B Biol Sci. 360:781–795.
Petrides M. 2007. The orbitofrontal cortex: novelty, deviation from expectation, and memory. Ann N Y Acad Sci. 1121:33–53.
Petrides M, Pandya DN. 1984. Projections to the frontal cortex from the posterior parietal region in the rhesus monkey. J Comp Neurol. 228:105–116.
Petrides M, Pandya DN. 1994. Comparative architectonic analysis of the human and the macaque frontal cortex. In: Boller F, Grafman J, editors. Handbook of neuropsychology. Amsterdam: Elsevier. p. 17–58.
Petrides M, Pandya DN. 1999. Dorsolateral prefrontal cortex: comparative cytoarchitectonic analysis in the human and the macaque brain and corticocortical connection patterns. Eur J Neurosci. 11:1011–1036.
Petrides M, Pandya DN. 2002. Comparative cytoarchitectonic analysis of the human and the macaque ventrolateral prefrontal cortex and corticocortical connection patterns in the monkey. Eur J Neurosci. 16:291–310.
Petrides M, Pandya DN. 2009. Distinct parietal and temporal pathways to the homologues of Broca's area in the monkey. PLoS Biol. 7:e1000170.
Picard N, Strick PL. 2003. Activation of the Supplementary Motor Area (SMA) during performance of visually guided movements. Cereb Cortex. 13:977–986.
Preuss TM, Goldman-Rakic PS. 1989. Connections of the ventral granular frontal cortex of macaques with perisylvian premotor and somatosensory areas: anatomical evidence for somatic representation in primate frontal association cortex. J Comp Neurol. 282:293–316.
Raos V, Evangeliou MN, Savaki HE. 2004. Observation of action: grasping with the mind's hand. NeuroImage. 23:193–201.
Raos V, Evangeliou MN, Savaki HE. 2007. Mental simulation of action in the service of action perception. J Neurosci. 27: 12675–12683.
Raos V, Kilintari M, Savaki HE. 2014. Viewing a forelimb induces widespread cortical activations. Neuroimage. 89:122–142.
Roy AC, Paulignan Y, Farne A, Jouffrais C, Boussaoud D. 2000. Hand kinematics during reaching and grasping in the macaque monkey. Behav Brain Res. 117:75–82.
Ruby P, Decety J. 2001. Effect of subjective perspective taking during simulation of action: a PET investigation of agency. Nat Neurosci. 4:546–550.
Saleem K, Logothetis N. 2007.A combined MRI and histology atlas of the rhesus monkey brain in stereotaxic coordinates. London, UK: Academic Press.
Savaki H. 2010. How do we understand the actions of others? By mental simulation, NOT mirroring. Cognitive Critique. 2: 99–140.

Savaki HE, Davidsen L, Smith C, Sokoloff L. 1980. Measurement of free glucose turnover in brain. J Neurochem. 35:495–502.

Savaki HE, Gregoriou GG, Bakola S, Moschovakis AK. 2015. Topography of visuomotor parameters in the frontal and premotor eye fields. Cereb Cortex. 25:3095–3106.

Savaki HE, Gregoriou GG, Bakola S, Raos V, Moschovakis AK. 2010. The place code of saccade metrics in the lateral bank of the intraparietal sulcus. J Neurosci. 30:1118–1127.

Savaki HE, Kennedy C, Sokoloff L, Mishkin M. 1993. Visually guided reaching with the forelimb contralateral to a "blind" hemisphere: a metabolic mapping study in monkeys. J Neurosci. 13:2772–2789.

Sawaguchi T, Yamane I, Kubota K. 1996. Application of the GABA antagonist bicuculline to the premotor cortex reduces the ability to withhold reaching movements by well-trained monkeys in visually guided reaching task. J Neurophysiol. 75:2150–2156.

Simone L, Rozzi S, Bimbi M, Fogassi L. 2015. Movement-related activity during goal-directed hand actions in the monkey ventrolateral prefrontal cortex. Eur J Neurosci. 42:2882–2894.

Sokoloff L, Reivich M, Kennedy C, Des Rosiers MH, Patlak CS, Pettigrew KS, Sakurada O, Shinohara M. 1977. The [^{14}C]-deoxyglucose method for the measurement of local cerebral glugose utilization: theory, procedure, and normal values in the conscious and anesthetized albino rat. J Neurochem. 28:879–916.

Stamos AV, Savaki HE, Raos V. 2010. The spinal substrate of the suppression of action during action observation. J Neurosci. 30:11605–11611.

Vogt S, Thomaschke R. 2007. From visuo-motor interactions to imitation learning: behavioural and brain imaging studies. J Sports Sci. 25:497–517.

Wang Y, Shima K, Isoda M, Sawamura H, Tanji J. 2002. Spatial distribution and density of prefrontal cortical cells projecting to three sectors of the premotor cortex. NeuroReport. 13: 1341–1344.

Yeterian EH, Pandya DN, Tomaiuolo F, Petrides M. 2012. The cortical connectivity of the prefrontal cortex in the monkey brain. Cortex. 48:58–81.